Determination of the seasonal mass balance of four Alpine glaciers since 1865

M. Huss,[1] A. Bauder,[1] M. Funk,[1] and R. Hock[2,3]

Received 28 March 2007; revised 17 August 2007; accepted 28 November 2007; published 1 March 2008.

[1] Alpine glaciers have suffered major losses of ice in the last century. We compute spatially distributed seasonal mass balances of four glaciers in the Swiss Alps (Grosser Aletschgletscher, Rhonegletscher, Griesgletscher and Silvrettagletscher) for the period 1865 to 2006. The mass balance model is forced by daily air temperature and precipitation data compiled from various long-term data series. The model is calibrated using ice volume changes derived from five to nine high-resolution digital elevation models, annual discharge data and a newly compiled data set of more than 4000 in situ measurements of mass balance covering different subperiods. The cumulative mass balances over the 142 year period vary between −35 and −97 m revealing a considerable mass loss. There is no significant trend in winter balances, whereas summer balances display important fluctuations. The rate of mass loss in the 1940s was higher than in the last decade. Our approach combines different types of field data with mass balance modeling to resolve decadal scale ice volume change observations to seasonal and spatially distributed mass balance series. The results contribute to a better understanding of the climatic forcing on Alpine glaciers in the last century.

Citation: Huss, M., A. Bauder, M. Funk, and R. Hock (2008), Determination of the seasonal mass balance of four Alpine glaciers since 1865, *J. Geophys. Res.*, *113*, F01015, doi:10.1029/2007JF000803.

1. Introduction

[2] Temporal glacier variations are among the clearest natural indicators of ongoing climate change [e.g., *IPCC*, 2007; *Oerlemans and Fortuin*, 1992]. A sound knowledge of the response of glaciers to climate change is of crucial importance for the assessment of water resources, sea level rise and natural hazards [e.g., *Haeberli*, 1995; *Zuo and Oerlemans*, 1997; *Kaser et al.*, 2006; *Huss et al.*, 2007]. In order to be able to predict the future reaction of alpine glaciers to climate change, we must understand their evolution in the past. Of several key parameters on glaciers, it is the mass balance which most clearly reflects climatic variation [*Oerlemans*, 1994; *Braithwaite and Zhang*, 2000; *Vincent*, 2002].

[3] Mass balance of alpine glaciers is dominated by two processes not directly related to one another: Accumulation is due to deposition of solid precipitation and contributes mainly to the winter balance of the glacier surface; ablation is determined by the melting of ice and snow, and dominates the summer balance. Conventional mass balance programs often do not distinguish between the two components [*Dyurgerov and Meier*, 1999]. However, seasonal values of mass balance provide the best insights to assess the effects of climatic forcing on glaciers. Mean specific mass balance can be biased by the dynamic response of the ice mass when the glacier shape and size is adapting to changed climatic conditions [*Jóhannesson et al.*, 1989]. Nevertheless, mean specific mass balance time series are of broad interest and have been determined in numerous glacier monitoring programs [*Dyurgerov and Meier*, 2005].

[4] Direct measurements of mass balance are available only for a limited number of glaciers and seldom extend far back in time. Numerical mass balance models can be applied in order to expand existing time series [e.g., *Torinesi et al.*, 2002; *Vincent*, 2002; *Machguth et al.*, 2006]. A variety of models relating measured climatic variables to glacier mass balance using different methods have been developed [*Braithwaite*, 1995; *Arnold et al.*, 1996; *Oerlemans et al.*, 1998; *Hock*, 1999, *Pellicciotti et al.*, 2005; *Gerbaux et al.*, 2005; *Steiner et al.*, 2005]. *Vincent* [2002] and *Vincent et al.* [2004] reconstructed the mass balance of four French glaciers over the 20th century using a simple degree-day model, but without calculating the spatial distribution of the mass balance. The model was calibrated using in situ mass balance measurements and ice volume changes. Results showed a significant increase in summer ablation during the last 20 years and a period of enhanced glacier recession in the 1940s. *Schöner and Böhm* [2007] calculated the mass balance evolution of glaciers in the Austrian Alps back to 1800 using regression equations and gridded data sets of meteorological variables.

[5] The aim of this study is to determine continuous time series of mean specific seasonal mass balance as well as the

[1] Versuchsanstalt für Wasserbau, Hydrologie und Glaziologie (VAW), ETH Zürich, Zürich, Switzerland.
[2] Geophysical Institute, University of Alaska Fairbanks, Fairbanks, Alaska, USA.
[3] Department of Earth Sciences, Uppsala University, Uppsala, Sweden.

Copyright 2008 by the American Geophysical Union.
0148-0227/08/2007JF000803

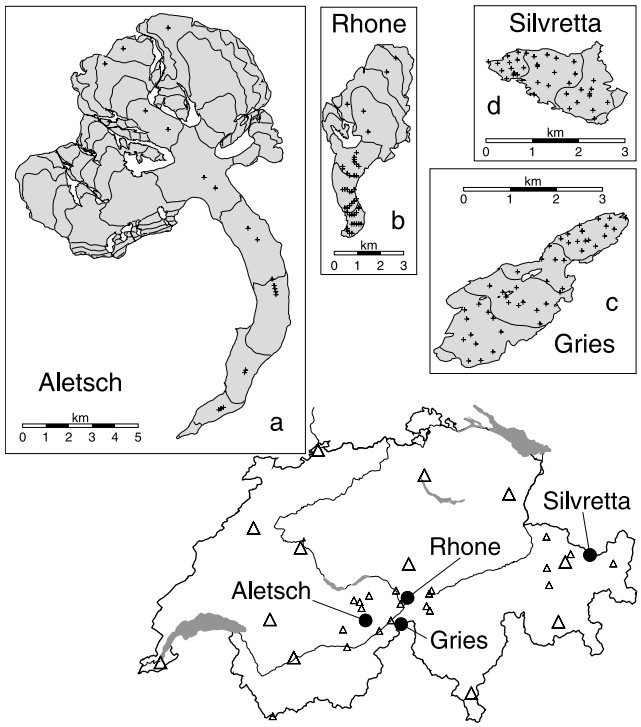

Figure 1. Location in Switzerland and outline of the four investigated glaciers. Triangles represent MeteoSchweiz weather stations. Large symbols indicate stations with continuous monthly air temperature and precipitation series since 1864 and small symbols refer to weather stations with shorter meteorological records of daily resolution. Note, that the scales of the glacier outlines in (a) and (b) differ from those in (c) and (d). The glacier extent is based on the latest DEM. The contour interval is 200 m, and crosses mark the position of mass balance stakes during the year 1980.

spatial distribution of mass balance of four well-documented glaciers in the Swiss Alps for the last 142 years. We extend the temporally limited mass balance series to the entire period since 1865, which marked the beginning of instrumental weather observations in Switzerland, and then resolve them into spatially distributed winter and summer balances. This provides a basis for the study of climate-glacier interaction in alpine environments and for the identification of processes that govern the mass balance evolution.

[6] We apply a numerical model as a tool for calculating seasonal glacier mass balances and merge all types of measurements which are accessible within the extensive glacier monitoring programs. The mass balance model is calibrated with ice volume changes which are known for all investigated glaciers from high-resolution digital elevation models (DEMs), a newly compiled data set of point-based mass balance measurements and discharge records. Using air temperature and precipitation data we resolve the ice volume changes given at a decadal scale to a seasonal scale and calculate the spatial distribution of mass balance on a regular grid. We derive the first complete seasonal mass balance time series for four Alpine glaciers for the 1865–2006 period. The results are backed up in an optimal way with numerous independent field data.

2. Study Sites and Field Data

[7] This study focuses on four glaciers in the Swiss Alps (Grosser Aletschgletscher, Rhonegletscher, Griesgletscher and Silvrettagletscher, Figure 1 and Table 1) for which exceptional data sets including extensive measurements of mass balance at stakes over several decades are available. The glaciers have different geometries, exposures and regional climate conditions and range in size from 3 to 80 km^2. Grosser Aletschgletscher is the largest ice mass in the European Alps. Whereas the local climate at the glacier terminus is relatively dry, high precipitation amounts are reported in the accumulation area owing to regional advection effects [*Schwarb et al.*, 2001]. Rhonegletscher is a south-exposed medium-sized valley glacier with a climatic setting similar to Aletsch. Griesgletscher is exposed to different meteorological conditions than the other three glaciers as it is situated south of the main Alpine crest. The small valley glacier has a north-eastern exposure. Silvrettagletscher is a small glacier in the north-eastern Swiss Alps with exposure to the west. The regional climate is characterized by relatively high precipitation amounts. The glaciers have lost between 16% (Aletsch) and 39% (Gries) of their area during the 20th century. Mass balance monitoring programs were set up on Griesgletscher and on Silvrettagletscher in the 1960s in the context of hydropower projects. The measurements on Aletsch and Rhonegletscher were conducted as part of glaciological research projects and data were usually too sparse to obtain area-averaged means.

[8] We use the following types of data for the modeling: (i) meteorological data, (ii) digital elevation models and ice volume changes, (iii) point-based mass balance measurements, and (iv) annual runoff volumes.

[9] We use different classes of climate data: Homogenized continuous monthly time series of temperature and

Table 1. Glacier Characteristics and Field Data Basis[a]

Glacier	Area[b] (km^2)	Elevation[b] (m a.s.l.)	Periods of Field Data			Number of DEMs, Years
			b_n	b_w	Q_a	
Aletsch	83.01	1560–4085	1921–2006	1921–2006	1923–2006	5 (1880, 1926, 1957, 1980, 1999)
Rhone	16.45	2197–3600	1885–1909, 1980–82	1980–1982	1895–1928, 1957–2006	6 (1874, 1929, 1959, 1980, 1991, 2000)
Gries	5.26	2410–3327	1961–2006	1994–2006	1957–2004	9 (1884, 1923, 1961, 1967, 1979, 1986, 1991, 1998, 2003)
Silvretta	2.89	2460–3073	1917–2006	1915–83, 2003–06	1934–2004	7 (1892, 1938, 1959, 1973, 1986, 1994, 2003)

[a]The time interval of available in situ measurements (b_n: surface net balance measured at stakes, b_w: surface winter balance) and discharge measurements (Q_a: annual runoff volume) are given.
[b]Based on the latest DEM available.

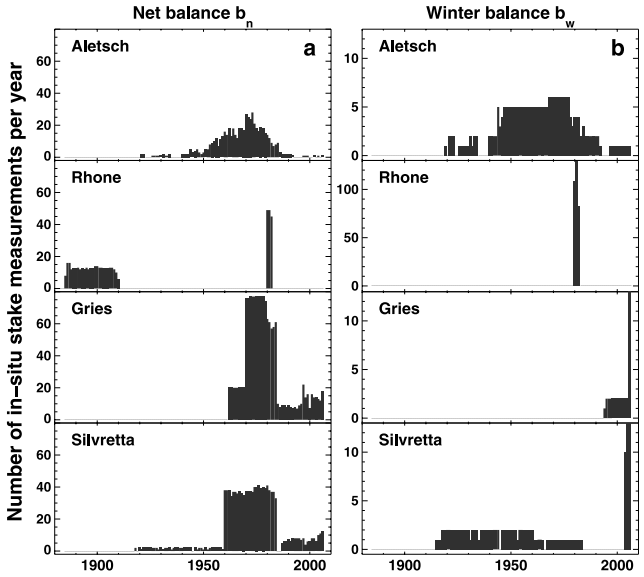

Figure 2. Number of in situ stake measurements per year for each glacier of (a) net mass balance and (b) winter mass balance.

precipitation since 1864 are available for 12 MeteoSchweiz stations [*Begert et al.*, 2005]. Twenty additional weather stations in the vicinity of the investigated glaciers provide information about the regional climate (Figure 1). These span shorter time periods but have daily resolution. High-alpine precipitation distribution information is provided by the PRISM data set (see section 3.3) compiled by *Schwarb et al.* [2001].

[10] For each glacier a set of five to nine high-resolution DEMs is available [*Bauder et al.*, 2007]. They cover the last century in decadal to semicentennial time periods (Table 1). DEMs for the period before 1960 are produced by the manual digitizing of topographic maps. The accuracy of the altitudinal information is estimated at ±5–10 m for digitized maps. The recent DEMs are based on photogrammetrical evaluation of aerial photographs. Their accuracy is ±0.3 m in the ablation zone, where the largest elevation changes occur, and ±1 m in the firn area [*Bauder et al.*, 2007]. The DEMs are interpolated to a regular grid of 25 m (50 m in the case of Aletsch). The DEMs provide a unique data basis for assessing long-term geometrical changes, in particular enabling ice volume changes to be calculated.

[11] During the last century mass balance measurements were conducted employing an enormous amount of manpower [e.g., *Aellen*, 1995]. Mass balance measurements mainly used for monitoring purposes have been performed on all four glaciers with varying intensity and during different subperiods of the 142 year study period (Figure 2). We evaluated all accessible data from reports and original field books and compiled a new digital data set of point-based mass balance measurements. It includes 3544 stake readings of surface net balance b_n and 773 measurements of surface winter balance b_w. Figure 2 shows the available data for each glacier. The uncertainty in direct measurements of net balance b_n at stakes is estimated as ±0.1 m water equivalent (w.e.) in the ablation area and may reach up to ±0.4 m w.e. in the accumulation area. An uncertainty of ±0.15 m w.e. is attributed to the measurement of winter balance b_w [*Gerbaux et al.*, 2005].

[12] Discharge records for the drainage basins are available, provided by the Swiss Federal Office for the Environment (Aletsch, Rhone and Silvretta). Runoff from the Gries catchment is determined based on water balance figures from a proglacial reservoir used for hydropower production. We use annual runoff volumes Q_a (Table 1). Their accuracy is estimated as ±5% (personal communication BAFU, 2007). The catchment basins of Aletsch, Rhone and Gries are more than 50% glacierized, whereas the Silvrettagletscher catchment is only 7% ice-covered.

3. Methods

3.1. Determination of Mass Balance

[13] We refer to two different types of mass balance: (i) point-based balance terms, and (ii) values integrated over the whole glacial area. All balance terms are specific quantities expressed in meters of water equivalent (m w.e.). $\overline{b_n}$ is the mean specific surface net balance that corresponds to the integrated sum of accumulation and ablation over the entire glacier over one year divided by that year's glacier surface area. $\overline{b_w}$ is the mean specific winter balance and $\overline{b_s}$ the mean specific summer balance. In this paper, $\overline{b_n}$ (1 Oct. – 30 Sept.), $\overline{b_w}$ (1 Oct.–30 April) and $\overline{b_s}$ (1 May–30 Sept.) are modeled quantities. b_n, b_w and b_s are the point-based specific net, winter and summer balances measured at a stake, respectively. The time interval corresponds to the effective dates of the readings. Accumulation and ablation on the glacier surface balance out at the equilibrium line. Its mean elevation is evaluated on 30th September each year and expressed in terms of the ELA (equilibrium line altitude).

[14] We calculate "conventional" mass balances [*Elsberg et al.*, 2001; *Harrison et al.*, 2005], i.e., the glacier area is updated annually. An annual time series of glacier area is obtained by linear interpolation of the glacier surface geometry between two successive DEMs. Using this technique both the annual change in glacier surface elevation and the change in glacier extent are estimated and step changes in the glacier geometry are avoided. The potential for error in this approach is low, as the measured DEMs constrain the interpolation in decadal intervals.

[15] The method for determining mass balance time series since 1865 is based on a surface melt model [*Hock*, 1999] coupled with a distributed accumulation model. The mass balance model calculates accumulation and ablation on a regular grid in daily time steps. Temperature and precipitation are the required input variables. The model is calibrated using ice volume changes, in situ mass balance measurements and discharge. In the following paragraphs each of the methodological steps is described in detail.

3.2. Ice Volume Changes

[16] The changes in ice volume provide an important basis for this study as they supply independent benchmarks for our approach which aid in determining the seasonal mass balance time series and in constraining the course of the calculated cumulative mass balance curve. By comparing two successive DEMs an ice volume change can be calculated. The imprecision of the volume change determination is less than 5% [*Bauder et al.*, 2007]. The ice volume

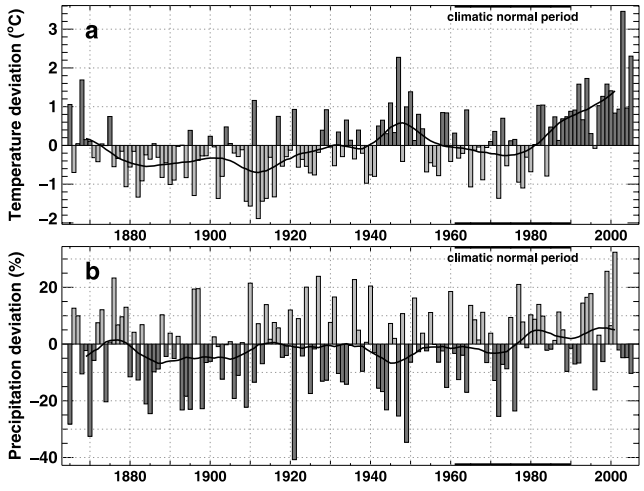

Figure 3. Homogenized time series of MeteoSchweiz: Mean deviations (12-station average) from the 1961–1990 climatic normal period of (a) summer temperature (May to September) and (b) annual precipitation. Solid curves indicate 10-year running means.

change is converted to water equivalent by assuming a constant ice density of 900 kg m^{-3}. For further information on this subject refer to *Bauder et al.* [2007].

3.3. Meteorological Time Series

[17] The mass balance model requires a continuous time series of daily air temperature and precipitation for the investigated period 1865–2006. As temperature and precipitation variables were not recorded at locations in immediate proximity to the glaciers, the measured data series needed to be scaled to the study sites. The procedures for the compilation of representative time series of temperature and precipitation are treated separately. In order to model the spatial distribution of mass balance accurately, the use of climatic data in high temporal resolution is essential. By adopting a daily time resolution, the short-term meteorological variability is taken into account, as for example, the height rise in the zero degree isotherm, albedo effects due to summer snow fall events, etc.

[18] Air temperature is relatively well correlated over large distances [*Begert et al.*, 2005] and can therefore be extrapolated with confidence. As temperature input we calculate a representative temperature time series for each glacier using the 12 homogenized data sets provided by MeteoSchweiz (Figure 3a). The time series are corrected for systematic biases which may be due, for example, to the relocation of the weather station or changed measuring techniques [*Begert et al.*, 2005]. The monthly temperature anomalies of the weather stations are averaged weighted with their inverse distance from the glacier.

[19] A local temperature lapse rate is determined for each month using weather stations within distances of less than 30 km to the glacier. Using these gradients, the glacier-specific homogenized temperature time series is shifted to the mean glacier elevation. The temperature data of monthly resolution thus obtained are downscaled by applying the daily fluctuations of the weather station at Bern.

[20] The distribution of precipitation in alpine environments is complex. Regional differences in precipitation are considerable, and altitudinal gradients of precipitation are variable over short horizontal distances [*Frei and Schär*, 1998; *Schwarb et al.*, 2001]. Measurements of precipitation over mountainous terrain are difficult and can be significantly biased by wind, especially in winter [*Sevruk*, 1985]. Hence the uncertainties are large regarding high alpine precipitation amounts.

[21] Because of the lack of precipitation data recorded close to the glaciers, we rely on a gridded precipitation map for obtaining a spatial distribution pattern of precipitation. The PRISM data set [*Schwarb et al.*, 2001] was generated using all available precipitation data in the Alpine region. It provides the monthly mean of precipitation sums during the period 1971–1990 on a grid of about 2 km. Interpolation of precipitation is conducted based on local altitudinal gradients determined by weighted regression between surrounding precipitation records [*Schwarb*, 2000].

[22] To obtain representative times series of high mountain precipitation we use daily data from the local weather station that correlate best with the winter snow water equivalent time series measured at stakes. The monthly precipitation sum recorded at this station is scaled to the values given by the PRISM data set for the glacier site. Thus the precipitation time series is composed of the temporal fluctuations of precipitation observed at a weather station near the glacier and the spatial distribution of precipitation sums given by the PRISM data set.

3.4. Model Description

[23] We calculate mass balance using an accumulation model coupled with a distributed temperature-index melt model [*Hock*, 1999]. This model elaborates on classical models using degree-day factors by varying these as a function of clear-sky direct radiation in order to account for the effects of slope, aspect and shading. Temperature-index models are based on a linear relation between positive air temperature and melt rate [e.g., *Braithwaite*, 1995; *Hock*, 2003]. *Ohmura* [2001] demonstrated that the physical base of temperature-index modeling is stronger than previously assumed. Melt is highly correlated with long-wave heat flux, for which air temperature is a good indicator. Temperature and precipitation at daily resolution are required input data which make the model applicable to centennial periods with poor spatial coverage of weather data. Daily surface melt rates M are computed for each cell of the DEM by:

$$M = \begin{cases} \left(F_{\mathrm{M}} + r_{\mathrm{ice/snow}} I\right) T & : \quad \mathrm{T} > 0 \\ 0 & : \quad \mathrm{T} \leq 0 \end{cases} \tag{1}$$

where F_{M} denotes a melt factor, $r_{\mathrm{ice/snow}}$ are radiation factors for ice and snow surfaces and I is the potential direct solar radiation. Because of the empirical character of the temperature-index model [*Hock*, 1999] the site-specific parameters F_{M} and $r_{\mathrm{ice/snow}}$ must be calibrated using field data.

[24] Air temperature at every grid cell is determined by a constant lapse rate. Precipitation is assumed to increase linearly with elevation (dP/dz). A correction factor accounts for gauge under-catch errors (C_{prec}) and a threshold temperature distinguishes snow from rainfall [*Hock*, 1999]. Discharge from the catchment basin is calculated as the sum of liquid precipitation and snow- and icemelt. It is

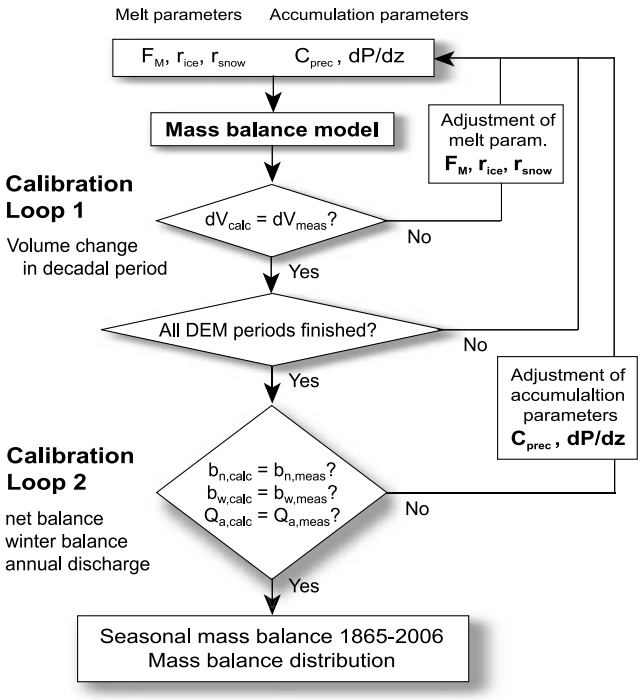

Figure 4. Calibration procedure. Melt parameters are calibrated for each subperiod given by two successive DEMs in Loop 1. Accumulation parameters are adjusted in Loop 2 for the entire 1865–2006 period.

corrected for evaporation by subtracting a constant value derived from basin characteristics [*Braun et al.*, 1994]. The spatial variation of accumulation on the glacier surface is influenced by snowdrift, avalanches and, for larger glaciers, by the regional precipitation field. The latter is evaluated based on the PRISM data set [*Schwarb et al.*, 2001]. To account for effects of avalanches and snowdrift we use slope and curvature derived from a DEM. We decrease accumulation linearly from 100 to 0% between a slope angle of 40° to 60°. Curvature is good indicator of regions with snow erosion and redeposition due to winds [*Blöschl et al.*, 1991] and is evaluated within a range of 200 m around each grid point. We multiply solid precipitation with a factor depending on curvature which varies between 0.5 and 1.5. A precipitation matrix is generated that describes the differential deposition of snow and is able to explain some of the complex patterns of accumulation in high mountain areas. Where measurements of the snow cover in individual years are available in high spatial resolution, the distribution map of solid precipitation is refined.

3.5. Model Calibration

[25] The calibration of our model is an automated multilayer iterative procedure. It is schematized in Figure 4. A wide range of field data originating from various sources is included. The procedure tunes the mass balances to the ice volume changes and minimizes the misfit between modeling results and in situ mass balance data and runoff.

[26] In calibration Loop 1 the calculated annual ice volume change is cumulated over each subperiod given by two successive DEMs of the glacier surface. Initialized by arbitrarily chosen values of C_{prec} and dP/dz the ice volume change is adjusted by varying the melt parameters F_M and $r_{ice/snow}$ to match the corresponding value determined geodetically (Figure 4). This calibration method integrates long-term overall changes of the glacier and does not depend on local effects of surface mass balance distribution. The procedure is repeated for all subperiods with available volume changes. Calibration Loop 2 adjusts the accumulation parameters (C_{prec}, dP/dz). Calibration Loop 1 and 2 are repeated until optimal agreement between both measured and modeled quantities is achieved. We minimize (1) the mean residual and (2) the standard deviation σ_d of the misfit between modeling results and independent in situ measurements of (i) point-based net balance b_n, (ii) point-based winter balance b_w and (iii) annual discharge volume Q_a.

[27] As precipitation parameters are atmospheric boundary conditions, they are assumed to be valid for the entire modeling period 1865–2006 (Figure 4). In contrast, for the melt parameters a different optimal set of parameters is obtained for each subperiod of consecutive DEMs. The subperiodical variations of the melt parameters are in the range of ±10% for each glacier. We assume the parameter combination of the first DEM subperiod to be valid for the two decades before the initial DEM. The parameters of the last period are used to model the mass balances after the last DEM acquired between 1999 and 2003. For this case the results are not constrained by measured ice volume change but can be corrected, if necessary, using the in situ measurements of b_n and b_w available for these years, with the exception of Rhonegletscher (Table 1).

[28] The calibration of the model using different types of in situ measurements is important. Both seasonal mass balance and the spatial distribution of mass balance could be in error if volume changes alone were used for calibration. By using the extensive data set of different field data types for calibration and validation of the results, we are able to resolve the ice volume change series seasonally and to determine a spatial distribution of the balance terms. Our results are well founded, based on independent field data of ice volume changes, in situ mass balance measurements and runoff volumes. The calculated and the measured quantities correspond well in most cases (Figure 5 and Table 2). The differences cluster in a zero-centered gaussian-shaped distribution (insets in Figure 5). To compare the runoff volumes of different catchment basins, the differences are normalized with the mean measured annual runoff $\overline{Q_a}$, and standard deviations $\sigma_{d,n}$ are given in percent (Figure 5 and Table 2).

[29] In the simultaneous minimization procedure to calibrate the mass balance model, an exact match of all classes of field data with the modeling results is usually not achievable (Figure 5). This is due to the inability of a numerical model to describe correctly all processes involved. Essentially, the model is tuned to the ice volume changes within each subperiod and the overall misfit is minimized between in situ measurements and model results.

4. Results

[30] We present four classes of results: (i) Cumulative time series of mean specific net balance, (ii) time series of mean specific winter, summer and net balance, (iii) the spatial distribution of mass balance and (iv) equilibrium line altitudes. By analyzing the model results, we identified four

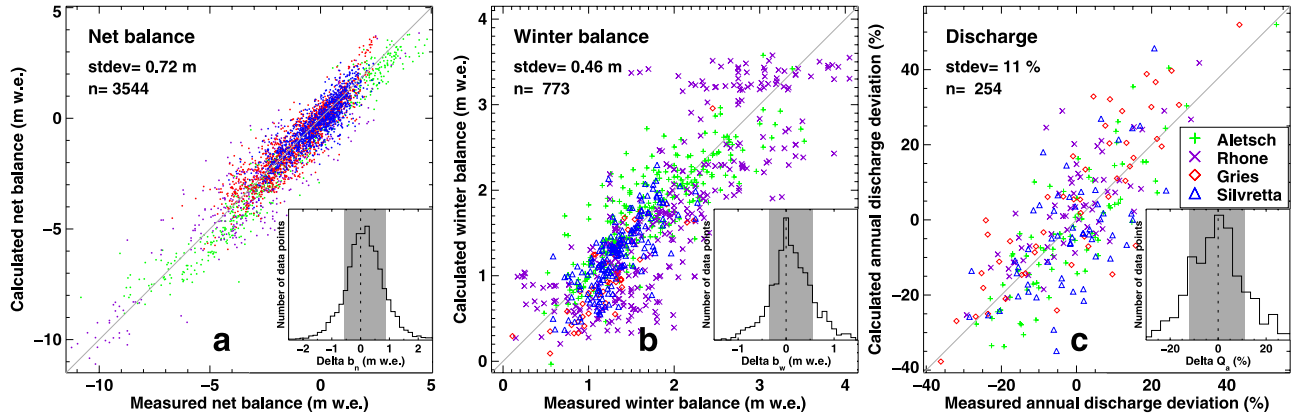

Figure 5. Comparison of measured and calculated (a) net mass balance b_n, (b) winter mass balance b_w at all available measurement locations, and (c) annual discharge volume Q_a normalized with the average runoff from the catchment. The standard deviation of the residuals between measured and calculated quantities, and the number of data points are stated. The distribution of the residuals is shown in the insets. The shaded bar corresponds to $\pm 1\sigma$ (containing 70% of the data points).

periods of decadal timescale with mass gain or exceptional rates of mass loss. The exact beginning and end of each period were set arbitrarily. Periods I (1912–1920) and III (1974–1981) are characterized by mass gains, Periods II (1942–1950) and IV (1998–2006) by extraordinarily high rates of mass loss. The mean specific net balances of each period differ significantly from the values of the entire time series (Student's t test at a significance level of 99%).

[31] The mass loss since 1865 is considerable for all glaciers analyzed. However, there are significant differences. The cumulative mass loss of Griesgletscher is three times greater compared to Silvrettagletscher (Figure 6 and Table 3). The cumulative mass balance curves show similar behavior during the entire study period. Aletschgletscher, Rhonegletscher and Griesgletscher are located within a distance of 30 km to each other, but their cumulative mass balances differ by a factor of more than 2.

[32] We averaged the mass balance series of the four investigated glaciers in order to investigate their year-to-year variability. Results are presented in Figure 7. Whereas winter balances display only minor changes during the last century, summer balances are subject to large fluctuations (Figure 7a). Mean specific net balances in the Periods I and III were slightly positive and led to advances of numerous glacier tongues [*Glaciological Reports*, 1881–2002]. The Periods II and IV are characterized by strongly negative mass balances (Table 4). Period IV includes 1998, 2003, and 2006, the years with the most negative net balances in the Swiss Alps determined within the conventional mass balance programs [*Glaciological Reports*, 1881–2002]. However, the mass balances in the 1940s (Period II) were more negative than those of Period IV (1998–2006). The results indicate that this is due to low winter balances during Period II (Figure 7b). Summer balances in Period IV are equally low as in the 1940s, but are partially compensated by relatively high amounts of winter precipitation. The two periods of mass gain are characterized by only slightly more winter accumulation, but significantly reduced melt in the summer months (Student's t test at a significance level of 99%). Summer balances are only half as negative as in the Periods II and IV (Figure 7). The most negative mass balance year since the end of the Little Ice Age was not

Table 2. Comparison of Model Results With Field Data[a]

	Net Balance		Winter Balance		Annual Discharge	
Glacier	n	σ_d, m	n	σ_d, m	n	$\sigma_{d,n}$ (%)
Aletsch	572	0.67	250	0.34	80	9.8
Rhone	423	1.16	318	0.58	66	10.1
Gries	1401	0.64	41	0.28	48	11.3
Silvretta	1148	0.57	164	0.27	60	13.3

[a]n is the number of data points, σ_d the standard deviation of the differences.

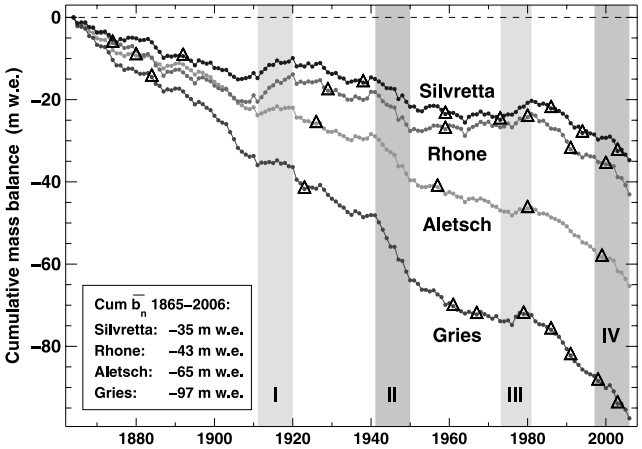

Figure 6. Time series of cumulative mean specific net balance (Cum $\overline{b_n}$) for Aletsch, Rhone, Gries and Silvretta in 1865–2006. Two decadal periods with positive (I, III) and strongly negative mass balances (II, IV) are highlighted. Triangles mark the years when DEMs are available. The model was calibrated so that ice volume changes obtained from integrating annual mass balances over the periods between consecutive DEMs coincided with those obtained from DEM differencing.

Table 3. Calculated Glacier Mass Balance Quantities: Cum $\overline{b_n}$ is the Cumulative Net Mass Balance Over the Period 1865–2006[a]

Glacier	Cum $\overline{b_n}$ (m w.e.)	$\overline{b_n}$	$\overline{b_w}$	$\overline{b_s}$ (m w.e. a^{-1})	db/dz (-)	$\overline{ELA}$ (m asl)
Aletsch	−65.3	−0.46	1.14	−1.60	0.0078	3003
Rhone	−43.0	−0.30	1.65	−1.95	0.0080	2944
Gries	−97.5	−0.69	1.32	−2.01	0.0088	2937
Silvretta	−34.7	−0.24	1.19	−1.43	0.0069	2811

[a] $\overline{b_n}$, $\overline{b_w}$, $\overline{b_s}$ are the mean specific net, winter and summer balances, db/dz the mass balance gradient in the ablation area and $\overline{ELA}$ the equilibrium line altitude averaged over 1865–2006.

Table 4. Calculated Mean Specific Mass Balances, ELA and AAR Averaged Over Periods I–IV and the Four Glaciers

Period	$\overline{b_n}$	$\overline{b_w}$	$\overline{b_s}$ (m w.e. a^{-1})	ELA (m a.s.l.)	AAR (%)
I (1912–1920)	0.36	1.56	−1.20	2793	65
II (1942–1950)	−1.19	1.14	−2.33	3076	34
III (1974–1981)	0.31	1.51	−1.20	2857	65
IV (1998–2006)	−0.96	1.36	−2.32	3066	41
1865–2006	−0.42	1.33	−1.75	2923	48

the year 2003 with its exceptional European summer heat wave [*Schär et al.*, 2004], but 1947.

[33] An important output of the model is the mass balance distribution. While comparison of two successive DEMs indicates only the elevation change at a given point which is determined by both mass balance and ice dynamics, we calculate effective rates of seasonal balance at every grid cell of 25 m (Figure 8). This makes it possible to determine the equilibrium line altitude (ELA), the accumulation area ratio (AAR) and the mass balance gradients directly from the gridded data sets. The model is able to reproduce the higher mass balance gradients in the ablation area. In the accumulation area a larger spread of mass balance is modeled which is due to the effects of snowdrift and avalanches (Figure 9).

[34] The mean specific net balance $\overline{b_n}$ is integrated over the annually updated glacier surface area, although the area cannot adapt immediately after a stepwise climate change. Therefore the dynamic response time of the glacier influences the values of mean specific mass balance [*Jóhannesson et al.*, 1989]. $\overline{b_n}$ is an indicator of the actual mass change and thus useful for hydrological and sea level change applications [*Harrison et al.*, 2005]. It also allows the intercomparison of different glaciers and represents the mass balance quantity usually determined within the framework of mass balance monitoring programs worldwide. The ELA, by contrast, is a quantity that is determined by climate and the aspect of the glacier. It is not influenced by glacier dynamics, extent and hypsometry, and thus reveals a largely unfiltered climatic signal.

[35] The annual variability of ELA is considerable (Figure 10). The lowest and the highest ELA values differ by 600 m. Even decadal mean ELAs show variations of up to 300 m between periods of positive and negative mass balances. The mean ELA was slightly higher in Period II than in Period IV. This implies that the greater mass losses in the 1940s are a climatic signal. The 1940s were warm and dry, whereas the most recent period is even warmer but wetter (Figure 3). The greater mass losses in Period II seem also to be favored by the larger glacier extents, i.e., lower-reaching glacier tongues. Some adaptation of the glaciers to the changed climatic conditions has taken place in the last century enabling the ice mass to be closer to equilibrium with higher ELAs (Figure 10).

5. Discussion

[36] The model approach used in this study is simple and well suited for long time periods. Glacier surface mass balance is determined using temperature and precipitation as input variables, but requires in situ measurements for calibration. The good agreement of measured and calculated

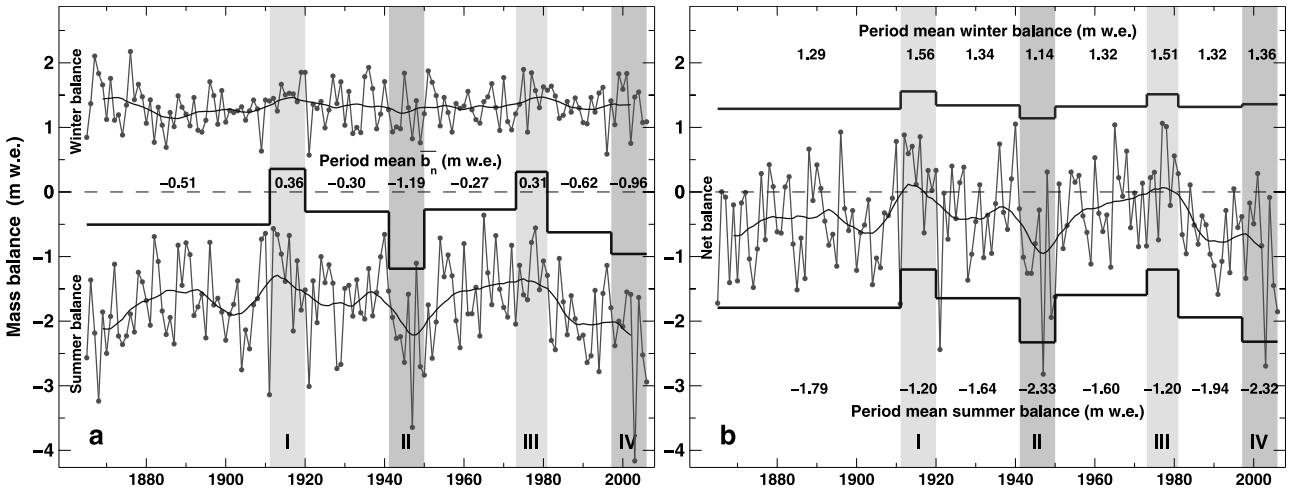

Figure 7. (a) Averaged seasonal mass balance series of Aletsch, Rhone, Gries and Silvretta, 1865–2006. Annual data points of winter balance $\overline{b_w}$ (positive) and summer balance $\overline{b_s}$ (negative) are smoothed using a 10-year running mean. The solid line shows the mean net balance in the four highlighted periods and in the interim. (b) Four-glacier average of surface net balances $\overline{b_n}$. The solid lines and the numbers correspond to the period means of winter and summer balance.

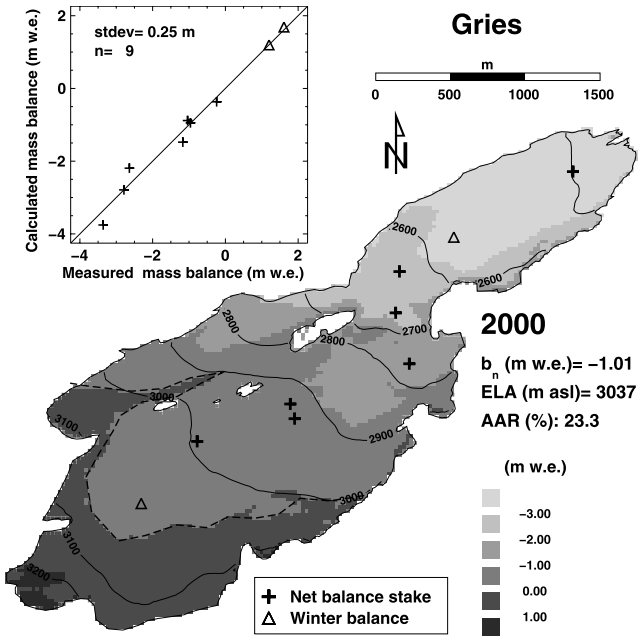

Figure 8. Spatial distribution of net balance as calculated for Griesgletscher in 2000. The dashed line follows the equilibrium line which is variable in altitude due to effects of aspect and snowdrift. Comparison of measured and calculated mass balance is shown in the inset.

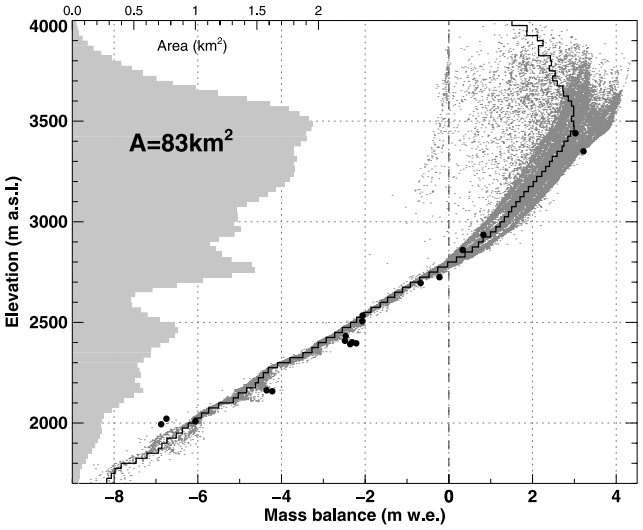

Figure 9. Altitudinal distribution of surface net balance as calculated for Grosser Aletschgletscher in 1977. Each small dot corresponds to one grid cell. The step function shows the mean net balance in elevation bands. Differences in the mass balance gradient and in the variability of mass balance between the ablation and the accumulation area are evident. Decreasing values of mass balance above 3500 m a.s.l. are due to effects of snowdrift and avalanches. Solid dots show in situ measurements of net balance. The area-elevation relation of the glacier surface is evaluated in 25 m elevation bands and is plotted in grey.

quantities indicate that the method presented has a potential in unifying all available data with modeling. Nevertheless, the applied model has some limitations: All variables of the energy balance other than air temperature are neglected.

[37] For example, albedo variations of the glacier surface as a result of snow metamorphism and dust deposition are insufficiently parameterized. Also variations in cloudiness may influence the melt rates substantially [*Pellicciotti et al.*, 2005] but are neglected in our approach. The relevance of these limitations, however, is larger for short timescales than for decadal periods. In the Swiss Alps, cloudiness was monitored at three high elevation sites for several decades [*Auer et al.*, 2007]. The data show no consistent trend or change during the two periods of accelerated glacier recession (Period II and IV) but a general trend toward more cloudiness. We refrain from including more meteorological input variables into the calculations since they are not available for the glacier sites and extrapolation procedures are doubtful. By calibrating a parameter set for each subperiod, constrained by a known ice volume change, the limitations discussed above are minimized. The values of the model parameters show a decreasing trend in the last decades which could be associated with the observed increase in global radiation after the 1980s [*Ohmura et al.*, 2007].

[38] The uncertainty of the calculated mass balance series depends critically on the quality of the DEM derived ice volume changes. However, since the individual DEMs are independent of each other, the imprecision of the ice volume change estimated as ±5% [*Bauder et al.*, 2007] does not propagate throughout the calculation period. In addition, the entire set of point-based mass balance and runoff measurements is used in the calibration procedure. Random errors in individual point measurements most likely cancel out within a large number of data points.

[39] Our method for determining mass balance time series of high temporal and spatial resolution is based on the meteorological input data. The knowledge about air temperatures in high alpine environments is relatively good, whereas little is known about the precipitation sum and its spatiotemporal distribution. Gridded data sets such as PRISM are known to have significant biases above

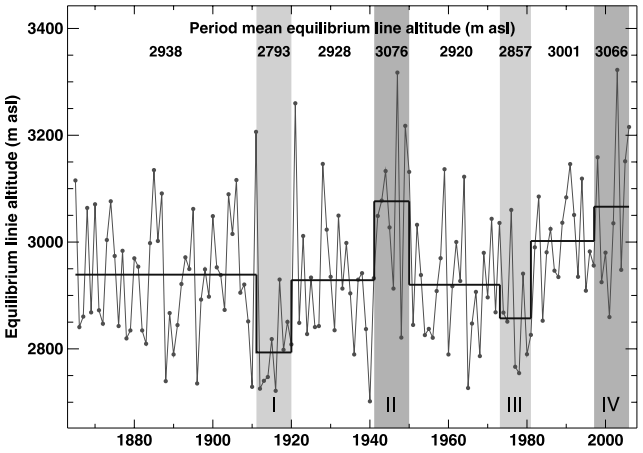

Figure 10. Annual ELAs averaged over Aletsch, Rhone, Gries and Silvretta. The solid line corresponds to the mean of ELAs in the Periods I to IV and in the interim.

2500 m a.s.l. [*Schwarb*, 2000; *Machguth et al.*, 2006]. This is due to the lack of reliable measurements of precipitation in high mountain terrain.

[40] Glaciers serve as precipitation gauges and could help to reduce this bias. The quality of the precipitation time series is assessed by comparison of the winter balance time series of individual stakes and the meteorological input of the model. Data of totalisators, precipitation gauges in high mountain areas, sampling annual to semi-annual precipitation sums, are available for some sites. However, they were rejected due to an inability to monitor data quality and measurement errors. The data set of point-based measurements of winter balance provides a possibility to enhance the knowledge about precipitation in areas relevant for glacier existence. In our model approach this is done in an iterative way by varying the precipitation correction factor C_{prec} until the model results are able to explain the measured winter balances. The precipitation of PRISM needs to be corrected by a factor of 1.3 for Rhonegletscher and by as much as 2.1 for Silvrettagletscher. Hence the in situ measurements contribute to reducing the uncertainty in the precipitation data. PRISM yields good estimates of the precipitation sum for Griesgletscher and for Grosser Aletschgletscher, however, it has to be corrected in the uppermost parts of the catchment for the latter.

[41] In order to evaluate the transferability of our approach to glaciers where only some of the independent field data types are available, we consider three cases of field data availability and their effect on the quality of the mass balance determination: (1) no field data, (2) only volume changes ΔV, (3) ΔV and net balance b_n, but no b_w data.

[42] 1. No field data: The method is doomed to fail in this case. The melt parameters of temperature-index models are site-specific and must be calibrated. They are not transferable within a sufficient range of confidence between individual glaciers. If it is possible, however, to calibrate the parameters during a number of years for an individual glacier, we may expect them to be valid for an extended period without data. This is what we assume for the years before the first DEM.

[43] 2. ΔV: If only field data of ΔV are available the model may be tuned to reproduce the observed decadal scale volume changes but for the wrong physical reasons. For example, overestimation of precipitation might be compensated for by overestimation of melt. There is no possibility to validate the distribution of the balance terms and their seasonal values because both accumulation and melt parameters can not be constrained unambiguously.

[44] 3. ΔV, b_n: The spatial distribution of net balance can be validated and fitted to the measurements (Figure 4). However, as for case 2 there is the risk of errors in winter and summer balances canceling out each other. We compared the mass balance series calibrated using only field data of ΔV and b_n to the reference time series obtained by considering all available measurements. The residuals of the mean specific net balance series show a standard deviation of $\sigma_d = 0.06$ m w.e. and the winter balances display a mean absolute deviation of $\Delta\overline{b_w} = 0.12$ m w.e. from the reference.

[45] We conducted a sensitivity test concerning the number of available in situ measurements. The data sets of b_n, b_w and Q_a were divided randomly into two groups of identical size. We obtained the almost identical results from the model calibration when applying either the first or the second of the reduced data sets.

[46] The field data series may be of irregular temporal and spatial coverage to be valuable to the calibration procedure. The quality of the seasonal mass balance series and their spatial distribution increases with the available types of field data. A large number of measurements within one class of calibration data and in particular its extensive temporal coverage leads to a high statistical weight of the data set.

[47] The differences in cumulative net mass balances over a period of one and a half century can be considerable for neighboring glaciers (Figure 6 and Table 3). This was already observed for other Alpine glaciers [*Kuhn et al.*, 1985]. The spatial representativity of single glacier mass balance records must be assessed carefully as they may be biased by, for example, ice dynamics and glacier surface geometry. A mean specific mass balance value determined for one glacier might not be representative for a whole mountain range. Cumulative mass balance series may diverge of various reasons: e.g., uneven changes in the local climate since 1865, different glacier hypsometries and topographic effects, different mass balance gradients, or the dynamic reaction of the ice mass. The relative contributions of these effects are not easy to determine and beyond the scope of this paper.

[48] Positive albedo feedback mechanisms may be another cause for the differential behavior of the investigated glaciers. Because of persistently negative mass balances, the firn line retreats, exposing ice surfaces with lower albedo. The albedo of the bare ice surface may change over time leading to further melt enhancement and increasing mass balance gradients. Our simple model approach is capable only of describing some of the albedo feedback mechanisms. More complex processes cannot be analyzed. The albedo feedback may be better able to explain the considerable mass losses in the 1940s that occurred in spite of lower summer temperatures than those experienced during the last two decades (Figure 3). Low winter accumulation and the succession of several extremely negative mass balance years caused the firn line to rise considerably, which reduced the albedo of the glacier surface and led to high melt rates.

6. Conclusion

[49] We present a method to resolve decadal to semicentennial ice volume changes obtained from repeated DEMs of the glacier surface to seasonal mass balance time series and to provide the spatial distribution of balance terms. The mass balance model requires only temperature and precipitation data which are widely available in the Alpine region as input. Our method incorporates all types of available in situ measurements in order to determine and analyze homogenized mass balance time series in seasonal resolution over centennial timescales tied directly to measured quantities. We are able to merge inhomogeneous or incomplete sets of field data covering different periods in varying density into time series of mean specific mass balances. Our approach allows direct comparison of the results from

different glaciers, since the periods of mass balance determination are exactly the same for all glaciers.

[50] We demonstrate that the mass balance evolution of four glaciers in the Swiss Alps has undergone significant fluctuations. Two decadal periods of mass gains are found, which are due to less negative summer balances. The general trend since 1865 is strongly negative, however, displaying large differences between neighboring glaciers. The most negative mass balances occurred in the 1940s. This is due to extraordinarily low winter accumulation and high summer temperatures. In future, we plan to extend the spatial coverage of the seasonal mass balance series to more than 20 glaciers in Switzerland in order to shed light on regional differences in high Alpine mass balance evolution. Our results emphasize the need to continue in situ mass balance measurements in seasonal resolution over long periods. We provide a promising method for combining these point measurements with geodetic observations and mass balance modeling to obtain mass balance quantities with high spatial and temporal resolution and extend measured mass balance series back in time.

[51] **Acknowledgments.** This work is supported by ETH Research Grant TH-17 06-1. Our results contribute to efforts in glacier monitoring. The weather data were recorded by MeteoSchweiz. The Federal Office for the Environment (BAFU) provided the runoff data. We thank Kraftwerke Aegina und Maggia AG for their support of the measurements on Griesgletscher. The immense contribution to mass balance measuring of previous researchers at the VAW is gratefully acknowledged. Swisstopo was responsible for the aerial photograph surveys. B. Nedela digitized old topographic maps and H. Bösch established DEMs from aerial photographs. We thank C. Frei for providing the PRISM data set and for helpful discussions. L.A. Rasmussen made valuable remarks on an earlier version of the manuscript. S. Braun-Clarke edited the English. The constructive comments of the scientific editor M. Church, the associate editor G. Hamilton, reviews by B. Brock and an anonymous reviewer substantially improved the clarity of the manuscript.

References

Aellen, M. (1995), Glacier mass balance studies in the Swiss Alps, *Zeitschrift für Gletscherkunde und Glazialgeologie*, *31*, 159–168.

Arnold, N. S., I. C. Willis, M. J. Sharp, K. S. Richards, and W. J. Lawson (1996), A distributed surface energy-balance model for a small valley glacier. I. Development and testing for Haut Glacier d'Arolla, Valais, Switzerland, *J. Glaciol.*, *42*(140), 77–89.

Auer, I., et al. (2007), HISTALP - Historical instrumental climatological surface time series of the Greater Alpine Region, *Int. J. Climatol.*, *27*(1), 17–46.

Bauder, A., M. Funk, and M. Huss (2007), Ice volume changes of selected glaciers in the Swiss Alps since the end of the 19th century, *Ann. Glaciol.*, *46*, 145–149.

Begert, M., T. Schlegel, and W. Kirchhofer (2005), Homogeneous temperature and precipitation series of Switzerland from 1864 to 2000, *Int. J. Climatol.*, *25*(1), 65–80, doi:10.1002/joc.1118.

Blöschl, G., R. Kirnbauer, and D. Gutknecht (1991), Distributed snowmelt simulations in an Alpine catchment, I: Model evaluation on the basis of snow cover patterns, *Water Resour. Res.*, *12*(27), 3171–3179.

Braithwaite, R. J. (1995), Positive degree-day factors for ablation on the Greenland ice sheet studied by energy-balance modeling, *J. Glaciol.*, *41*(137), 153–160.

Braithwaite, R. J., and Y. Zhang (2000), Sensitivity of mass balance of five Swiss glaciers to temperature changes assessed by tuning a degree-day model, *J. Glaciol.*, *46*(152), 7–14.

Braun, L. N., M. Aellen, M. Funk, R. Hock, M. B. Rohrer, U. Steinegger, G. Kappenberger, and H. Mueller-Lemans (1994), Measurement and simulation of high alpine water balance components in the Linth-Limmern head watershed (north-eastern Switzerland), *Zeitschrift für Gletscherkunde und Glazialgeologie*, *30*, 161–185.

Dyurgerov, M., and M. Meier (1999), Analysis of winter and summer glacier mass balances, *Geografiska Annaler*, *81*(4), 541–554.

Dyurgerov, M. B., and M. F. Meier (2005), Glaciers and the changing earth system: a 2004 snapshot, *Occasional Paper 58*, Institute of Arctic and Alpine Research, University of Colorado, pp. 117.

Elsberg, D. H., W. D. Harrison, K. A. Echelmeyer, and R. M. Krimmel (2001), Quantifying the effects of climate and surface change on glacier mass balance, *J. Glaciol.*, *47*(159), 649–658.

Frei, C., and C. Schär (1998), A precipitation climatology of the alps from high-resolution rain-gauge observations, *Int. J. Climatol.*, *18*(8), 873–900, doi:10.1002/(SICI)1097-0088(19980630)18:8<873::AID-JOC255>3.0.CO;2-9.

Gerbaux, M., C. Genthon, P. Etchevers, C. Vincent, and J. Dedieu (2005), Surface mass balance of glaciers in the French Alps: Distributed modeling and sensitivity to climate change, *J. Glaciol.*, *51*(175), 561–572.

Glaciological Reports (1881–2002), The Swiss Glaciers, 1880–2000/01, Yearbooks of the Glaciological Commission of the Swiss Academy of Sciences (SCNAT), published since 1964 by the Laboratory of Hydraulics, Hydrology and Glaciology (VAW) of ETH Zürich, http://glaciology.ethz.ch/swiss-glaciers/.

Haeberli, W. (1995), Glacier fluctuations and climate change detection-Operational elements of a worldwide monitoring strategy, *WMO – Bull.*, *44*(1), 23–31.

Harrison, W. D., D. H. Elsberg, L. H. Cox, and R. S. March (2005), Different mass balances for climatic and hydrologic applications, *J. Glaciol.*, *51*(172), 176.

Hock, R. (1999), A distributed temperature-index ice- and snowmelt model including potential direct solar radiation, *J. Glaciol.*, *45*(149), 101–111.

Hock, R. (2003), Temperature index melt modelling in mountain areas, *J. Hydrol.*, *282*(1–4), 104–115, doi:10.1016/S0022-1694(03)00257-9.

Huss, M., S. Sugiyama, A. Bauder, and M. Funk (2007), Retreat scenarios of Unteraargletscher, Switzerland, using a combined ice-flow mass-balance model, *Arct. Antarct. Alp. Res.*, *39*(3), 422–431.

IPCC (2007), Climate Change 2007. The scientific basis. Contributions of Working Group I to the Forth Assessment Report of the Intergovernmental Panel on Climate Change, *Tech. rep.*, WMO/UNEP, Cambridge University Press.

Jóhannesson, T., C. Raymond, and E. Waddington (1989), Time-scale for adjustment of glaciers to changes in mass balance, *J. Glaciol.*, *35*(121), 355–369.

Kaser, G., J. G. Cogley, M. B. Dyurgerov, M. F. Meier, and A. Ohmura (2006), Mass balance of glaciers and ice caps: Consensus estimates for 1961–2004, *Geophys. Res. Lett.*, *33*(19), L19501, doi:10.1029/2006GL027511.

Kuhn, M., G. Markel, G. Kaser, U. Nickus, F. Obleitner, and H. Schneider (1985), Fluctuations of climate and mass balances: Different responses of two adjacent glaciers, *Zeitschrift für Gletscherkunde und Glazialgeologie*, *21*(1), 409–416.

Machguth, H., F. Paul, M. Hoelzle, and W. Haeberli (2006), Distributed glacier mass balance modelling as an important component of modern multi-level glacier monitoring, *Ann. Glaciol.*, *43*(1), 335–343.

Oerlemans, J. (1994), Quantifying global warming from the retreat of glaciers, *Science*, *264*(5156), 243–245, doi:10.1126/science.264.5156.243.

Oerlemans, J., and J. P. F. Fortuin (1992), Sensitivity of glaciers and small ice caps to greenhouse warming, *Science*, *258*(5079), 115–117, doi:10.1126/science.258.5079.115.

Oerlemans, J., B. Anderson, A. Hubbard, P. Huybrechts, T. Johannesson, and W. Knap (1998), Modelling the response of glaciers to climate warming, *Clim. Dyn.*, *14*(4), 267–274.

Ohmura, A. (2001), Physical basis for the temperature-based melt-index method, *J. Appl. Meteorol.*, *40*(4), 753–761.

Ohmura, A., A. Bauder, H. Müller, and G. Kappenberger (2007), Long-term change of mass balance and the role of radiation, *Ann. Glaciol.*, *46*, 367–374.

Pellicciotti, F., B. J. Brock, U. Strasser, P. Burlando, M. Funk, and J. Corripio (2005), An enhanced temperature-index glacier melt model including the shortwave radiation balance: Development and testing for Haut Glacier d'Arolla, Switzerland, *J. Glaciol.*, *51*(175), 573–587.

Schär, C., P. L. Vidale, D. Lüthi, C. Frei, C. Häberli, M. A. Liniger, and C. Appenzeller (2004), The role of increasing temperature variability in European summer heatwaves, *Nature*, *427*, 332–336.

Schöner, W., and R. Böhm (2007), A statistical mass-balance model for reconstruction of LIA ice mass of glaciers in the European Alps, *Ann. Glaciol.*, *46*, 161–169.

Schwarb, M. (2000), The Alpine Precipitation Climate, Ph.D.thesis, ETH-Zürich, no. 13911.

Schwarb, M., C. Daly, C. Frei, and C. Schaer (2001), Mean annual and seasonal precipitation throughout the European Alps 1971–1990, *Tech. rep.*, Hydrological Atlas of Switzerland, plates 2.6, 2.7.

Sevruk, B. (1985), Correction of precipitation measurements, in Workshop on the Correction of Precipitation Measurements, Zürich, Switzerland, pp. 13–23, WMO/IAHS/ETH.

Steiner, D., A. Walter, and H. J. Zumbühl (2005), The application of a nonlinear backpropagation neural network to study the mass balance of the Great Aletsch glacier, *J. Glaciol.*, *51*(173), 313–323.

Torinesi, O., A. Letrguilly, and F. Valla (2002), A century reconstruction of the mass balance of Glacier de Sarennes, French Alps, *J. Glaciol.*, *48*(160), 142–148.

Vincent, C. (2002), Influence of climate change over the 20th Century on four French glacier mass balances, *J. Geophys. Res.*, *107*(4375), (D19), 4375, doi:10.1029/2001JD000832.

Vincent, C., G. Kappenberger, F. Valla, A. Bauder, M. Funk, and E. L. Meur (2004), Ice ablation as evidence of climate change in the Alps over the 20th century, *J. Geophys. Res.*, *109*(D10), D10104, doi:10.1029/2003JD003857.

Zuo, Z., and J. Oerlemans (1997), Contribution of glacier melt to sea-level rise since AD 1865: a regionally differentiated calculation, *Clim. Dyn.*, *13*(12), 835–845, doi:10.1007/s003820050200.

A. Bauder, M. Funk, and M. Huss, Versuchsanstalt für Wasserbau, Hydrologie und Glaziologie (VAW), ETH Zürich, 8092 Zürich, Switzerland. (mhuss@vaw.baug.ethz.ch)

R. Hock, Geophysical Institute, University of Alaska Fairbanks, 903 Koyukuk Drive, Fairbanks, AK 99775-7320, USA.